We are IntechOpen, the world's leading publisher of Open Access books Built by scientists, for scientists

4,800
Open access books available

122,000
International authors and editors

135M
Downloads

Our authors are among the

154
Countries delivered to

TOP 1%
most cited scientists

12.2%
Contributors from top 500 universities

CLARIVATE ANALYTICS BOOK CITATION INDEX INDEXED

WEB OF SCIENCE™

Selection of our books indexed in the Book Citation Index in Web of Science™ Core Collection (BKCI)

Interested in publishing with us?
Contact book.department@intechopen.com

Numbers displayed above are based on latest data collected.
For more information visit www.intechopen.com

11

A Low Cost Anticollision Reader

Dan Tudor Vuza[1], Reinhold Frosch[2], Helmut Koeberl[2] and Damien Boissat[2]
[1]*Institute of Mathematics of the Romanian Academy,*
[2]*Frosch Electronics OEG, Graz,*
[1]*Romania,*
[2]*Austria*

1. Introduction

The chapter presents some aspects related to the design of a low cost anticollision reader based on the HTRC110 reader chip from NXP Semiconductors (NXP Semiconductors, 2006 a) and the AT91SAM7S64 controller from Atmel.

The HTRC110 reader chip was mainly intended for integration into systems that need to identify one single RFID tag at a time. At the request of the host the chip sends the adequate command to the tag, retrieves the answer of the latter in analog form, digitizes the data and offers to the host the data retrieved from the tag in binary format. The chip does not provide support for collision detection and anticollision identification procedures in case that several tags in the antenna field respond to the same command at the same time.

Nevertheless, the chip does provide access to the analog demodulated signal representing the response sent by the tags via load modulation of the carrier. This access was meant by the producer for the purposes of antenna tuning and testing. In the present design, it is by exploiting this feature that one achieves the anticollision functions.

In section 2 of the chapter one describes the general configuration of the reader at block level, and particularly how the internal ADC of the AT91SAM7S64 controller is used for converting the test signal of the HTRC110 chip to numeric format and what signal-processing procedures are used for extracting the bit information from the signal and detecting collisions on bit positions. Included is also a brief description of the communication facilities of the reader with a host PC, such as RS232, USB and wireless.

In section 3 one addresses some aspects of the concern whether the analog signal provided by the HTRC110 chip is adequate enough for collision detection. The main point here is that, while the other members of the anticollision readers produced by Frosch Electronics use constant amplitude current drive for the antenna and they decode the antenna voltage variations caused by load modulation at the tag, in the present case the HTRC110 chip uses constant amplitude voltage drive and it decodes the voltage variations at the junction between the antenna coil and the tuning capacitor. Because of this, the load modulation employed by the tag causes transients in the reader antenna that are longer than in the current drive case and are directly influenced by the antenna Q. In turn these transients cause the demodulated signal from the tag to have slower raising/falling edges than in the current drive case, which may interfere with collision detection if these transients are too long. It is the purpose of the section to analyze the dependence on Q of this effect and to compare it with the current driven case.

Source: Development and Implementation of RFID Technology, Book edited by: Cristina TURCU,
ISBN 978-3-902613-54-7, pp. 554, February 2009, I-Tech, Vienna, Austria

The next two sections complement the discussion of transients exposed in section 3. In section 4 one shows how these transients can be simulated with the aid of Spice and observed in isolated form, that is, separated from the signal on which they are superimposed. Section 5 presents the tag simulator, which can be a useful tool for the designer assisting him in the process of antenna Q optimization.
Finally, section 6 describes how besides anticollision identification of several tags, the reader was also designed for identification of a single tag in public B mode, according to ISO standards 11784 and 11785 for animal identification. The problem is here that the tag sends its data in a continuous and cyclic manner, without needing any reader command, so the alignment of the bit boundaries with respect to the reader clock is not known in advance to the reader. A bit synchronization procedure is needed and one such procedure is described in the section.

2. Description of the reader

Figure 1 presents the block schematic of the new reader. The signal lines connecting the HTRC110 chip to our design are divided into three groups. The lines in the first group are connected to the antenna circuit as explained in the next section. The lines in the second group, Clock, Data In and Data Out, are digital lines and serve to the exchange of binary information with the Atmel AT91SAM7S64 micro-controller (uC). The lines in the third group represented as dashed on the figure form the "non-standard" group as they are related to our particular design and would not be present in the standard usage intended by the producer.

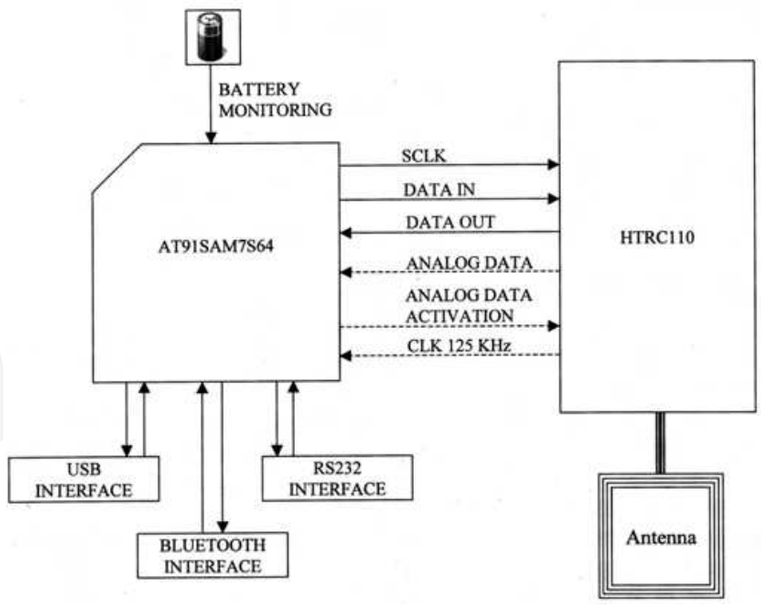

Fig. 1. Block schematic of the reader.

The HTRC110 chip may work with carrier frequencies of 125 KHz or 134 KHz. The antenna circuit provides both the power to the tags and the communication with the latter. Commands are sent to tags by 100% modulation of the carrier. The Data In line may be used by uC for modulating the carrier between on and off. A command to the tags is sent as a

sequence of bits, each bit consisting of a space followed by a mark. The carrier is off during spaces and on during marks. A longer mark corresponds to a one, a shorter one to a zero. In our design, we use one of the internal uC timers for setting the duration of a mark. During marks, the timer is clocked by signal coming from one of the antenna drivers of the HTRC110 chip. During spaces, the timer is clocked from one of the frequency generators of uC since the carrier is off. The timer is programmed to generate an interrupt to uC after a certain number of clocks; the interrupt routine writes the Data In line of the HTRC110 chip with the appropriate value and programs number of clocks after which the next interrupt should be triggered.

So far this is standard usage of the HTRC110 chip. For us the significant part starts with the reception of the answer from the tags. The tags send their answer at a command from the reader by switching an internal load. The bits are encoded as shown in figure 2. When communicating with a single tag, Manchester (MC) encoding is used. Anticollision encoding (AC) is used when responses from several tags are expected. However, the HTRC110 chip was mainly intended for communication with a single tag and for this reason it has no provision for collision detection. In a standard usage, after demodulating and filtering the tag response, the chip digitizes it according to being lower or higher than a certain threshold and presents to the host this binary version of the signal on the Data Out line. The host has thus access to only a part of the information contained in the analog signal. In the absence of collisions, this information should suffice, in principle, for recovering the answer from the tag. The detection of collisions would be however quite questionable without having full access to the analog signal.

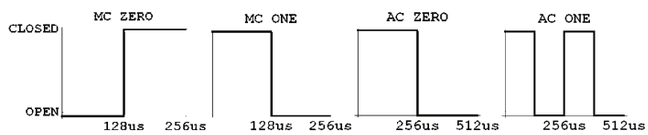

Fig. 2. Waveforms for Manchester (MC) and Anti-collision (AC) bit encoding. The Y-axis indicates the state of the tag switch.

Our design takes advantage of the test line provided by the producer of the HTRC110 chip. After a certain activation procedure is performed, the test line gives access to the analog output of the demodulator and filter. This access was intended to be useful especially for maintenance procedures, such as antenna tuning and testing. In our case, we use it for getting access to the tag response in analog form. For this purpose, the test line is connected to one of the 8 channels of the internal analog-to-digital converter (ADC) of uC. The signal coming from the antenna driver goes to another internal timer of uC where its frequency is divided by two. The ADC is programmed to use the output of the named timer as the start of conversion signal. Thus one sample of the analog signal is taken every two carrier cycles.

Following a command from the reader, the tag starts sending its answer after a certain number of carrier cycles since the end of the command, specified by the producer. Again by using the uC timer for counting carrier cycles, our reader waits for that specific number, after which the automatic recording of the tag answer starts by programming the interface between ADC and the internal RAM memory of uC. With its 16 Kbytes of RAM, uC provides plenty of storage space for the tag answer. After having recorded the latter, uC decodes it by computing the correlations between each bit and the encoding waveforms shown in figure 2. Let us consider here the AC encoded case. Denote by C_0 and C_1 the

absolute values of the correlations between a certain bit and the AC waveforms for zero and one, and let C_{max} and C_{min} be the greater and the lower of C_0 and C_1 respectively. The uC firmware considers that a response has been indeed received if C_{max} exceeds some threshold, in which case the bit in question equals zero or one according to whether C_0 is greater or lower than C_1. A collision on that bit is considered to have occurred if the ratio C_{min}/C_{max} exceeds the collision threshold. In such situation, the reader sends more selective commands until a collision-free response from a single tag is received. With the aid of anticollision algorithms based on this principle, all tags in the antenna field are identified by the reader. All computations are done exclusively with integers and therefore are fast enough, so the timing requirements of the identification procedures are mainly determined by the tags without significant overhead added by uC.

Figure 3 left shows a sequence of bits in analog format together with their digitized form that would be provided by the HTRC110 chip in a standard usage. One can distinguish in the figure the AC coded bits 0, 1, 0, 0, 1, 1, 0, 1. Figure 3 right shows the same sequence but the 4-th, 5-th and 6-th bits are now affected by collisions. One sees that there is hardly any difference in the digitized output; so this signal cannot be used for collision detection. On the other hand, the collision ratios C_{min}/C_{max} as computed from the analog signal for the bits in question are 0.274, 0.629, 0.621 for the collision case and 0.002, 0.032, 0.035 for the collision-free case, the presence of collisions being thus identified without any doubt.

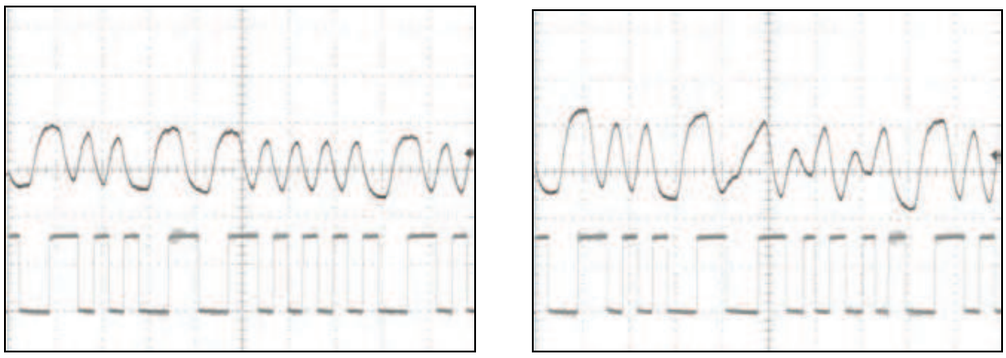

Fig. 3. Baseband signal demodulated by reader. Data from tags received without collisions (left) and with collisions (right).

Our reader provides communication with a host PC via three channels: RS232, USB and wireless. The RS232 channel facilitates the connection to a PC serial port; the serial protocol is supervised by the embedded serial interface of uC and needs an on-board component that translates between the logic levels employed by the uC and PC serial ports. The Bluetooth wireless module is connected to the RS232 channel and realizes the conversion between the serial and wireless protocols. No additional component is needed for the USB channel since all the protocol is managed by one of the embedded peripherals of uC.

The reader may be powered either by battery or from the PC via USB cable. A 3.3V regulator provides the power to the HTRC110 chip, the uC and to all other components on-board. When powered from battery, another channel of the ADC is used for monitoring the battery voltage. During the intervals when the ADC is not used for decoding the answer from tags, a sample of the battery voltage is periodically taken. The uC monitors these samples and triggers an alarm in the form of a blinking led when the voltage starts going low; it can also send these samples at the request of the host PC if it is wished to display the battery voltage on the screen.

In figure 4 one sees the reader being driven by a program run on a personal digital assistant. The communication between the latter and the reader is wireless. The computer screen shows the result of identifying three tags with the anticollision algorithm.

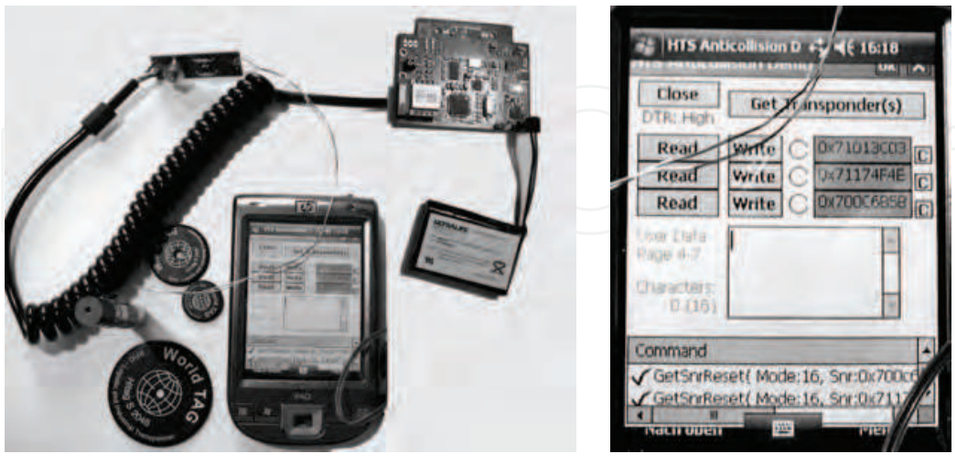

Fig. 4. The low cost reader driven by a PDA via wireless communication (left) and the screen of the PDA showing the result of identifying three tags (right).

3. Effects of transients on data reception

The reference book on RFID (Finkenzeller, 2003) discusses the influence of the reader antenna quality factor Q. A high Q leads to high current, hence larger reading distance. On the other hand, a too high Q would limit the bandwidth for transmission and reception. This means that transmission and reception act both in the direction of imposing an upper bound on Q. Since these processes are based on different effects, one cannot expect that the constraints they impose would be similar; in fact they can be quite dissimilar, as we shall see. In the mentioned book one gives an estimation formula for Q based on the constraints imposed by transmission, with just a few hints about how to proceed for reception. In the following we shall analyze the influence of Q on the process of reception by the method of transients. We shall see that, from the point of view adopted here, there is a fundamental difference between the so-called voltage driven readers and current driven readers as far as the constraints imposed by reception are concerned. The example reader design of (Finkenzeller, 2003) is a voltage driven reader, as it is the low cost reader discussed now; current driven readers are produced by Frosch Electronics and seems to be less known, therefore it would be worthwhile to be analyzed here.

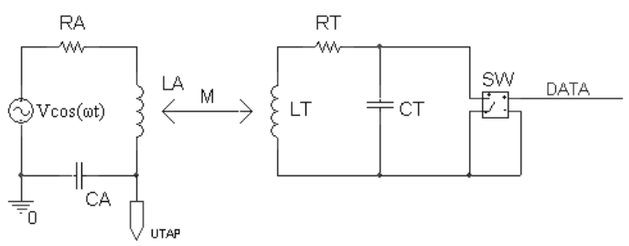

Fig. 5. Interaction between reader and tag.

Consider the principle schematic of the reception circuit of the low cost reader as shown in figure 5. During reception, the reader powers the antenna with a sinusoidal voltage of constant amplitude at the carrier frequency of f_C = 125 KHz. The tag transmits data by opening and closing the switch SW, which, due to the magnetic coupling M, modulates the current through the antenna. The reader senses the current modulation (or equivalently, the modulation of the voltage across an impedance traversed by the antenna current, such as the voltage U_{TAP}) and extracts the baseband signal that contains the data.

In the following we shall use the letter s as the argument in the Laplace transform. Denoting by U_A the driving voltage, by I_T the current flowing into the tag coil and by Z_T the impedance seen by the tag coil, we have the following relations:

$$U_A(s) = \left(R_A + L_A s + \frac{1}{C_A s} \right) I_A(s) + MsI_T(s),$$
$$-Z_T(s)I_T(s) = LsI_T(s) + MsI_A(s).$$

By eliminating I_T we find the antenna current and the voltage at the tap point in function of the antenna voltage and the tag impedance:

$$I_A(s) = \frac{U_A(s)}{R_A + L_A s + \frac{1}{C_A s} - \frac{M^2 s^2}{L_T s + Z_T(s)}}, \quad U_{TAP} = \frac{I_A(s)}{C_A s}. \tag{1}$$

The impedance Z_T is formed by the tag coil resistance R_T in series with the parallel combination of the resonance capacitor C_T and the resistance of the switch R_{SW}. In the following we shall consider only tags tuned to the carrier frequency. Using the equalities $L_A C_A = L_T C_T = (\omega_C)^{-2}$ where $\omega_C = 2\pi f_C$ and introducing the coupling constant $k^2 = M^2/L_A L_T$, the antenna quality factor $Q_A = L_A\omega_C/R_A$, the series and parallel quality factors of the tag $Q_s = L_T\omega_C/R_T$, $Q_p = R_{SW}/L_T\omega_C$ and the frequency normalized Laplace variable $x = s/\omega_C$, we arrive at

$$U_{TAP}(s) = \frac{P_T(x)}{P_A(x)P_T(x) - k^2 x^2 (x^2 + Q_p^{-1} x)} U_A(s) \tag{2}$$

where

$$P_A(x) = x^2 + Q_A^{-1} x + 1,$$
$$P_T(x) = x^2 + (Q_p^{-1} + Q_s^{-1})x + Q_p^{-1} Q_s^{-1} + 1.$$

We are interested to see what happens to U_{TAP} when the tag changes the state of the switch SW. This can be inferred from the following general principle. Consider a circuit described by the linear system

$$\frac{dX(t)}{dt} = SX(t) + Y\exp(j\omega t) \tag{3}$$

where X is the vector of the state variables and $Y\exp(j\omega t)$ is a harmonic signal that drives the circuit. The general solution of such a system is the sum between the harmonic solution $(j\omega - S)^{-1}Y\exp(j\omega t)$ and the general solution of the homogeneous system, for which $Y = 0$. Assuming the circuit stable, the solution of the homogeneous system will approach zero and will therefore represent the transient part of the complete solution. Now assume that some change in the matrix S happens at time t_0, such as opening or closing a switch that would cause a change in the component parameters and/or the configuration of the system. Suppose that $X(t)$ is a solution of (3) up to t_0. After t_0, the state vector of the circuit will evolve according to system (3′) obtained from (3) by replacing S with the new matrix S'. The new vector $X'(t)$ is uniquely determined by solving (3′) with the initial condition $X'(t_0) = X(t_0)$. As before, $X'(t)$ will be the sum between the new harmonic solution $(j\omega - S')^{-1} Y\exp(j\omega t)$ and a transient solution uniquely determined by the initial condition. As times goes past t_0, the evolution of the state vector will approach the harmonic solution. Thus, the change of configuration at moment t_0 results in changing the evolution of the system from one harmonic solution to another, but has also the side effect that transients will manifest themselves for some time after the change. The time constants of these transients are determined by the linear system in effect *after* the change, that is, system (3′). As well known from Laplace transform theory, if one is interested in the time constants of the transients that affect an output of the system, one has to look for the roots of the denominator of the transfer function from the driving input to that output and take the inverses of the real parts of those roots, provided that the degree of the denominator equals the order of the system (in order to be sure that the denominator includes all characteristic roots of the system).

In the case of our reader, we see that when the tag acts on the switch SW, U_{TAP} will be affected by a transient whose time constants are computed by finding the roots of the denominator $P(x)$ of the transfer function in (2). Specifically, for any such root x_0, $-1/(\omega_C \operatorname{Re} x_0)$ will be the time constant for a transient. In the following we shall consider the limiting case of small coupling constants k, which is the usual case in real situations. With this assumption, the roots of $P(x)$ will be in close vicinity of the roots of the equation $P_A(x)P_T(x) = 0$. There are now two cases to be distinguished. In the first case, the tag closes the switch. Two of the time constants are determined by the roots of P_A while the other two are determined by the roots of P_T after having substituted Q_p with its value corresponding to the closed state of the switch. Since R_{SW} is low in the closed state, the time constants determined by P_T will be short, leaving the transients determined by P_A to manifest themselves for a longer time. In other words, when the tag closes the switch, the transients affecting U_{TAP} will be mainly determined by the quality factor of the reader antenna. In the second case, the tag opens the switch. Since Q_p is high in this case, $P_T(x)$ essentially reduces to $x^2 + Q_s^{-1}x + 1,$ an expression similar to $P_A(x)$. In other words, transients due to both the reader antenna and to the tag will be present; which of them will be longer depends on how the quality factor of the reader antenna compare to the series quality factor of the tag resonant circuit.

The above conclusions can be confirmed by experiment. Figures 6 and 7 show the voltages on U_{TAP} of our voltage-driven reader measured with a digital oscilloscope and displayed in Spice. Since a real tag would not allow for a clear display of the transients, these were obtained with the tag simulator to be described in section 5, which imitates a real tag by using the same electrical model as in figure 5. The switch pulse in figures 6 and 7 is the

pulse applied at the data line of the switch in figure 5. For a better display of transients, the named figures show the envelopes of the voltages on U_{TAP} obtained by joining the maxima over positive half cycles; the voltage itself is shown in figure 6, which corresponds to the case of normal working conditions. In this case, the measured value of Q_A was found to be 9.45; this was done by measuring U_{TAP} when no tag was present and using the relation $Q_A = |U_{TAP}|/|U_A|$, which follows from (2) by substituting $x = j$ and $k = 0$ (one has also to take into account that, for an antenna circuit driven by a square pulse that toggles between U_{MAX} and $-U_{MAX}$, the amplitude U_A of the sinusoidal voltage source in our model is found to be 1.27 U_{MAX} by Fourier analysis). In figure 7, Q_A has been lowered to 1.41 by inserting an additional 162 Ohms resistance in the antenna circuit. One sees that the transient after closing the switch has been greatly shortened, confirming thus that this transient is mainly due to the reader antenna. On the other hand, the transient after opening the switch could not be reduced below 100 μs since it is mainly determined by Q_s of the tag when the transient due to the reader is short.

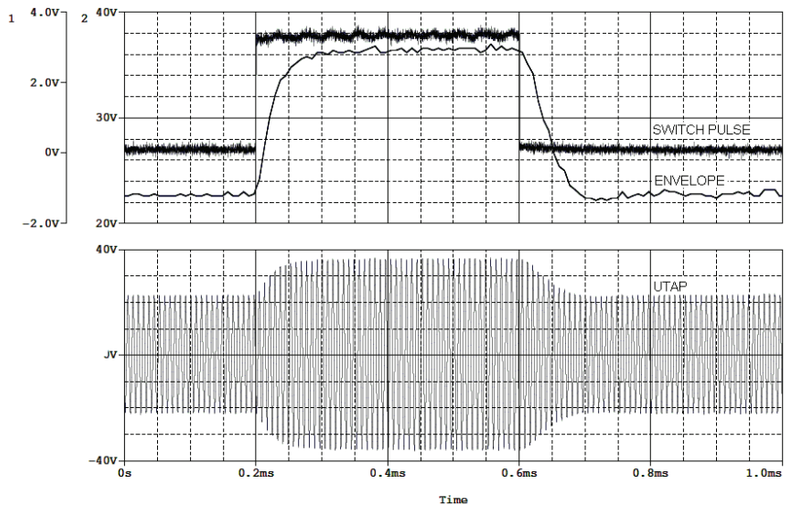

Fig. 6. Transients on U_{TAP} of the voltage-driven reader for normal Q_A.

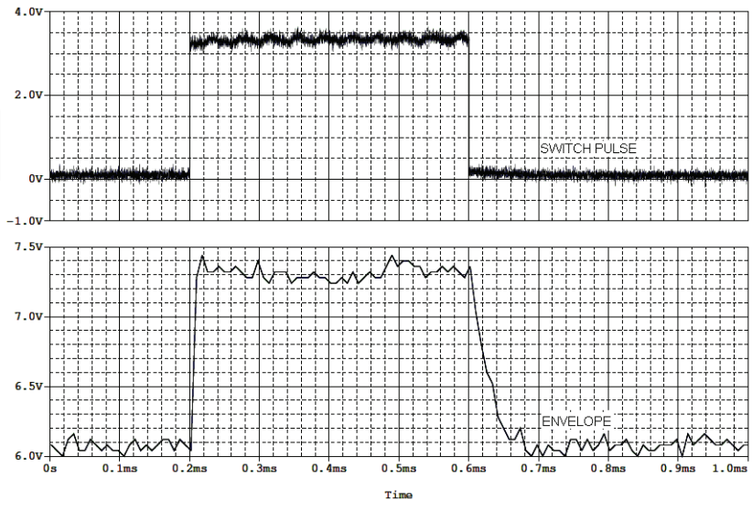

Fig. 7. Transients on U_{TAP} of the voltage-driven reader for lowered Q_A.

When k is small and the quality factors are not too small, the transients oscillate with a frequency close to f_C. Consequently they pass through the filters of the reader receiver and are demodulated, resulting in a baseband signal with slower transitions between the states corresponding to the open and closed positions of the tag switch. If the time constants of the transients are comparable to the duration of the bits transmitted by the tag, deleterious effects on bit decoding and especially on collision detection can result, since such transients can distort the waveforms that encode the bits. Therefore, an upper bound of the reader antenna quality factor Q_A should be imposed. By the above discussion, any decrease in Q_A will shorten the transient that occurs when the tag closes the switch. This will be true only to lesser extent for the transient after the opening of the switch: even if Q_A is made very low so that the transient due to the reader antenna vanishes quickly, there still remains the effects of the transient related to the serial quality factor Q_s of the tag.
From the above discussion, it is advisable that the 95% - 5% decrease time of the antenna transient, equal to 2.94 times its time constant, should be less than the smallest interval T_{SW} between changes of state of the tag switch. The time constant being equal to $2Q_A/\omega_C$, it results that the following upper bound should be imposed on Q_A:

$$Q_A \leq \frac{\pi f_C T_{SW}}{2.94}.$$

For our reader, T_{SW} = 128 μs, corresponding to the case of Manchester encoding. It follows that an upper bound of 17 should be imposed on Q_A.
It is interesting to compare the above situation with that of other readers designed or produced by Frosch Electronics for which the antenna circuit is not voltage driven but current driven (Frosch Electronics, 2004; Gelinotte et al., 2006; Vuza et al., 2007). For those readers, it is the amplitude of the antenna current that is kept constant by the reader during reception, the action of the tag on the switch resulting in the modulation of antenna voltage that is sensed and decoded by the reader. In figure 5, one replaces the voltage source by a current source and instead of U_{TAP} one senses the voltage U_A across the current source. From (1) and (2) one obtains

$$U_A(s) = \frac{P_A(x)P_T(x) - k^2x^2(x^2 + Q_p^{-1}x)}{\omega_C C_A x P_T(x)} I_A(s). \tag{4}$$

One may think that the above method would not apply, since the degree of the denominator is less that the order four of the system; and moreover the root $x = 0$ would seem to suggest an infinite time constant. However, on closer look, we see that the current through L_A and the voltage across C_A do not count as state variables, as far as the transients caused by load modulation are concerned. Indeed, the former is fixed by the current source, while the latter is determined by the current source and the initial voltage at system start. The remaining state variables are attached to L_T and C_T so that the order of the system is two, not four. Rewriting (4) as

$$U_A(s) = \frac{P_A(x)}{\omega_C C_A x} I_A(s) - \frac{k^2x^2(x + Q_p^{-1})}{\omega_C C_A P_T(x)} I_A(s), \tag{5}$$

we see that only the second term in the right hand matters, the first term being independent of the part of the system where the state variable are located. The conclusion is that the time constants of transients are here completely determined by the tag and are neither dependent on the antenna circuit nor on the coupling. The antenna quality factor Q_A has no influence on the reception transients.

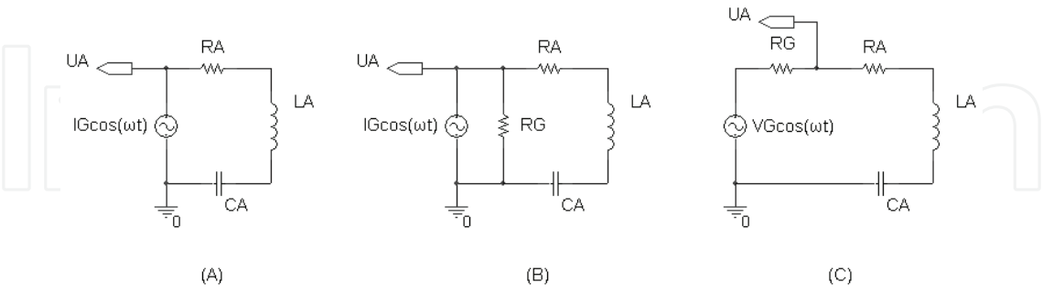

Fig. 8. Current driven reader: ideal current source (A), non-ideal current source (B), Thévenin equivalent of non-ideal current source (C).

The above argument is correct for an ideal current source. A non-ideal current source has a resistance R_G across it. We may replace the source, as in figure 8, by its Thévenin equivalent consisting of a voltage source producing the voltage $U_G = R_G I_G$ in series with resistance R_G. When this replacement is made, the current driven reader has been transformed into a voltage driven reader to which the above discussion apply; one has only to notice that R_A is now replaced by the composite resistance $R_A + R_G$. The current driven reader senses the voltage U_A across the antenna, which in our case equals $U_G - R_G I_A$. The expression for I_A in function of U_G is obtained by multiplying by $C_A s$ the voltage U_{TAP} from (2), in which we have replaced $P_A(x)$ by $R_G \omega_C C_A x + P_A(x)$ in order to take into account the composite resistance. After simplifications the result is

$$U_A(s) = \frac{P_A(x)P_T(x) - k^2 x^2 (x^2 + Q_p^{-1} x)}{R_G \omega_C C_A x P_T(x) + P_A(x)P_T(x) - k^2 x^2 (x^2 + Q_p^{-1} x)} R_G I_G(s).$$

As R_G grows larger, the denominator is essentially dominated by its first term and hence becomes less and less dependent on Q_A and k. In the limit of R_G growing to infinity, the above expression reduces to (4), as it should.
The conclusion is that, in the case of current driven readers, the process of reception imposes fewer restrictions on Q_A, amounting to no restriction at all for the limiting case of an ideal current source. Therefore, the upper bound of Q_A of such a reader is mainly imposed by the transmission.

4. Spice simulation of reception transients

As discussed above, the transients in the solution of the system (3) caused by switching from S to S' are obtained by subtracting the periodic solution corresponding to system S' from the actual solution. By using this principle one can display the reception transients in Spice. In figure 9, T, T0 and T1 are hierarchical blocks that model tags; each of them is coupled, with the same constant k, to a voltage driven reader. The model for the tag is the same as in figure 5. The inputs of those blocks correspond to the data lines that drive the switches. Through

the simulation, blocks T0 and T1 have their switches set to the open and closed positions respectively; the switch of block T is changed from open to closed and back to open. After a short interval from the beginning of the simulation, the voltages $U_{TAP,0}$ and $U_{TAP,1}$ of the readers coupled to T0 and T1 will stabilize to the periodic solutions corresponding to the respective positions of their switches. The transient on voltage U_{TAP} of the reader coupled to T caused by closing the switch is then obtained by subtracting $U_{TAP,1}$, the periodic solution for the closed switch, from U_{TAP}, which is effected by the difference block in the figure. Similarly, the transient on U_{TAP} caused by opening the switch is obtained by subtracting $U_{TAP,0}$ from U_{TAP}.

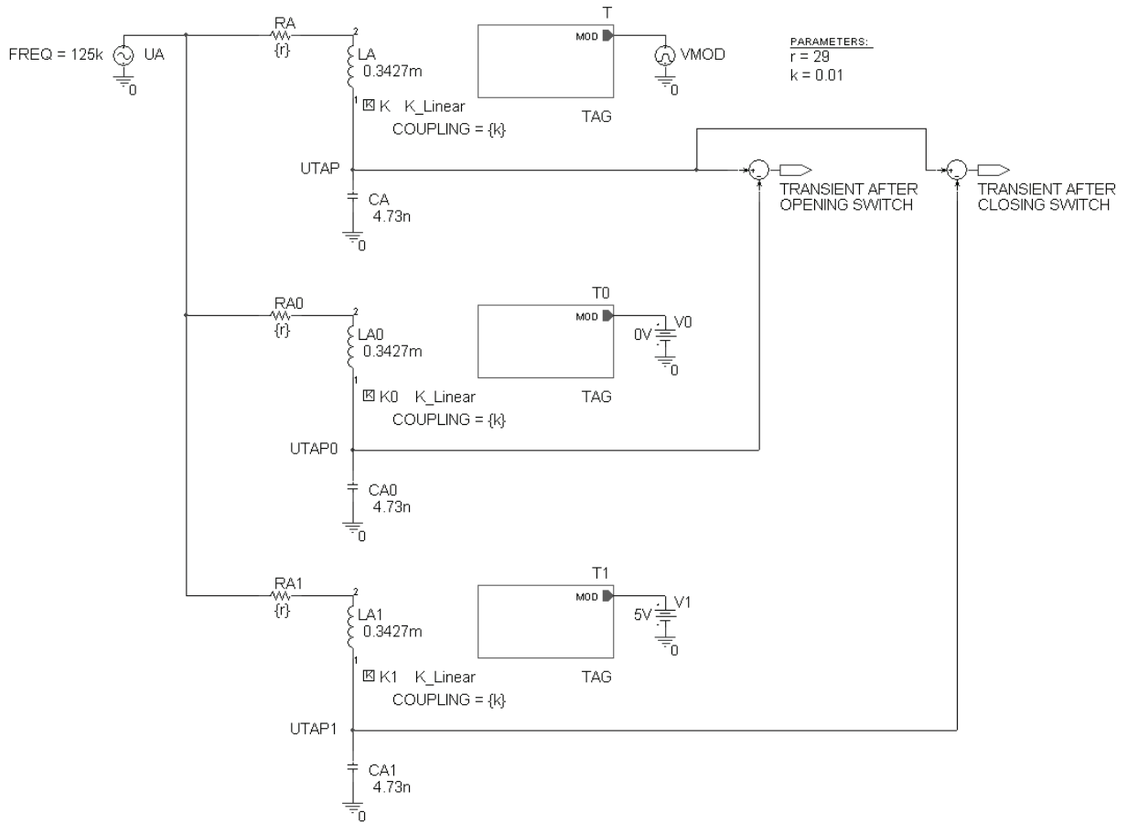

Fig. 9. Spice schematic for simulation of reception transients.

Figures 10 and 11 show the results of the simulations. In both figures, a value of 12.73 was used for Q_s; the switch was closed at time 2 ms and opened at time 3 ms. Figure 10 corresponds to a high value of 67.29 for Q_A. One sees that the transient after switch closing, which is due mainly to the reader antenna, resembles closely the transient after switch opening, with the exception of the first 100 μs when the transient due to the tag also manifests itself. This is confirmed by the simulation of figure 11 where a low value of 1.35 was used for Q_A. One sees that the transient after switch closing is indeed very short, while the transient after switch opening, which is now mainly determined by Q_s of the tag, lasts for about 100 μs. As a check, the 95% - 5% decrease time corresponding to Q_s is

$$2.94\frac{2Q_s}{\omega_C} = 95.3 \text{ μs}.$$

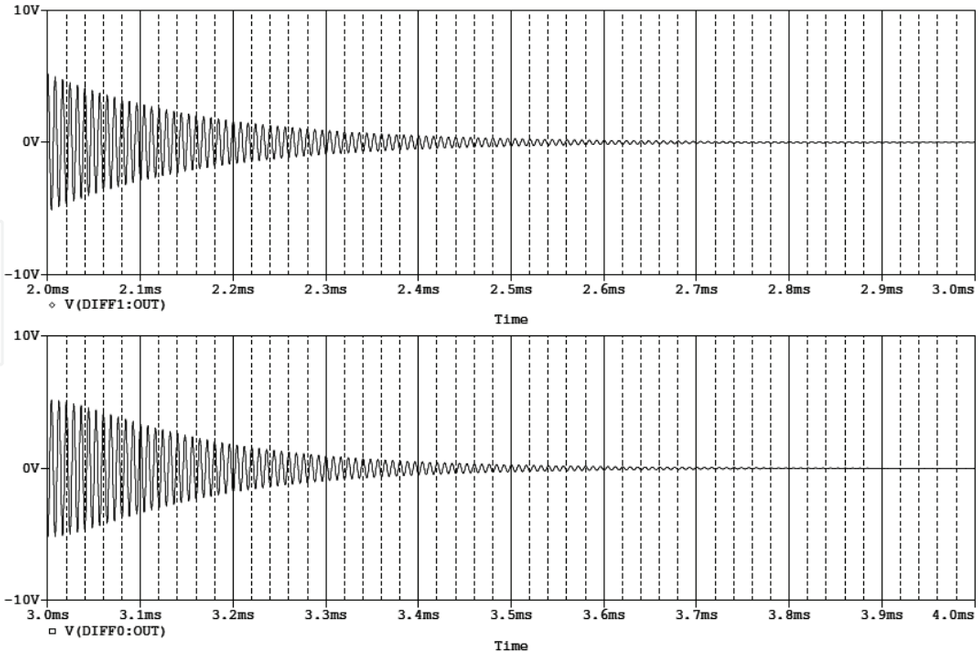

Fig. 10. Simulated transients for high Q_A.

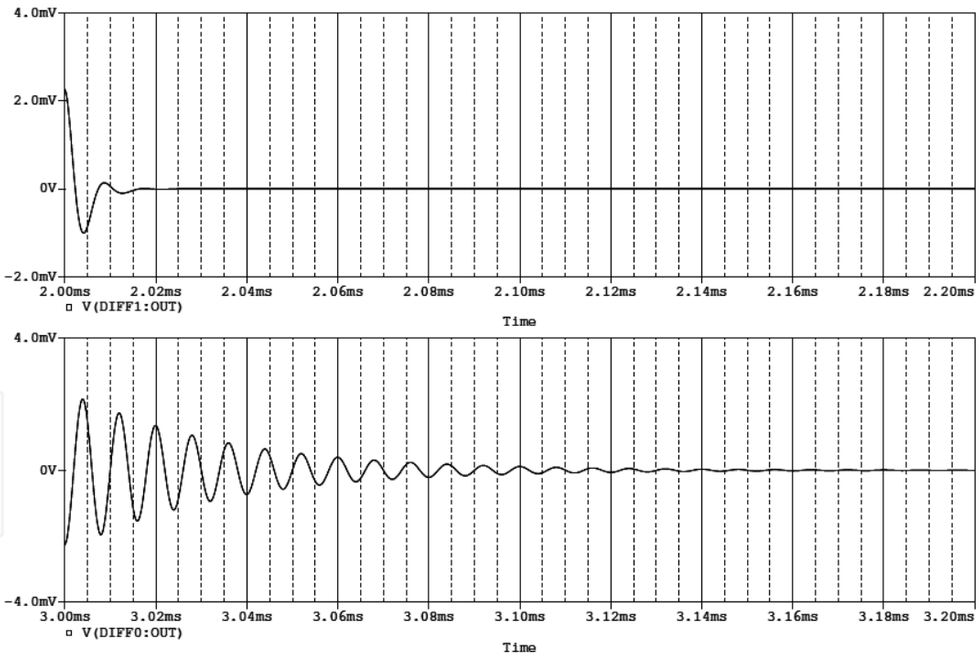

Fig. 11. Simulated transients for low Q_A.

5. A short description of the tag simulator

An ongoing cooperation between NXP Semiconductors and Frosch Electronics targets the development of a reader for a new member of the Hitag family of RFID transponders complying with the ISO/IEC 18000 standard. Since at the time of the reader development

the tag itself was under development, a simulator has been designed in order to substitute the real tag and simulate the communication between reader and as many tags as needed. With its aid, several fast identification algorithms have been designed and tested on the reader.

Figure 1 presents the principle schematics of the tag simulator, which is built around the evaluation board for the Atmel AT91SAM7S64 micro-controller (uC). In the figure the simulator is interacting with a reader and its antenna.

For the purpose of receiving the commands intended for tags, two logic signals of the reader, namely the signal that drives the carrier modulator and the output of the carrier generator, are connected to two inputs of uC. Via the former signal uC is made aware of carrier interruption during spaces; the latter signal clocks one of the internal timers of uC with the aid of which uC counts the carrier cycles during marks, just as the tag would do.

The simulator transmits data to the reader via load modulation, by switching in and out resistor *RM*. This causes the variation of the current through the simulator coil *L* placed near the reader antenna, which results in modulating the voltage on the reader antenna via magnetic coupling *M*. Thus, from the electrical viewpoint, data transmitted by the simulator appears to the reader as if transmitted by a real tag, since the principle of load modulation employed by the latter is also used with the simulator.

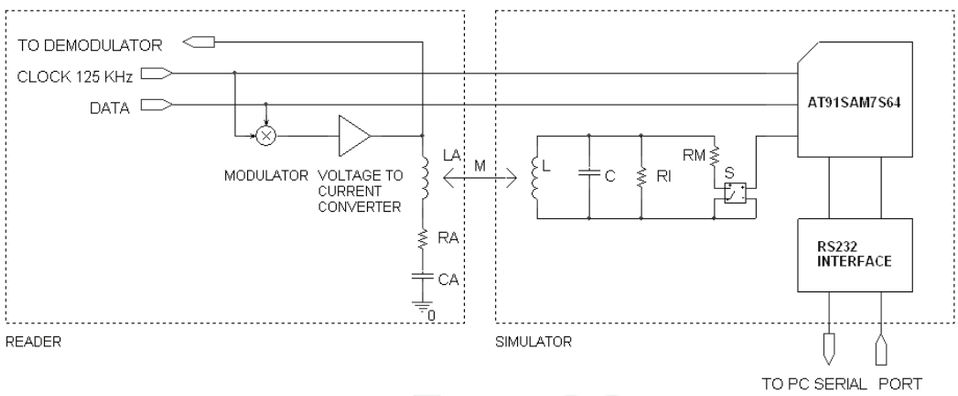

Fig. 12. The simulator and its interaction with a reader.

The uC keeps in its internal RAM a list of all tags to be simulated. Each tag is represented as a record containing the serial number and the status of the tag that can be powered off, active or halted. When responding to a Get ID command, the uC first builds the list of tags that in reality would respond to the command. Then, for every bit position of the response to be sent, uC looks whether the tags included in the list would transmit the same bit or not. In the former case, uC transmits that common bit according to the AC load modulation waveforms of figure 13. In the latter case, uC uses a modulation waveform called Collision in the named figure. At the reader, the reception of such a waveform will be interpreted as a collision, since it has a strong correlation with the encoding waveforms for both a zero and a one. In this way, the reader will be in the same situation as when receiving data simultaneously from several tags and collisions are detected on some bit positions.

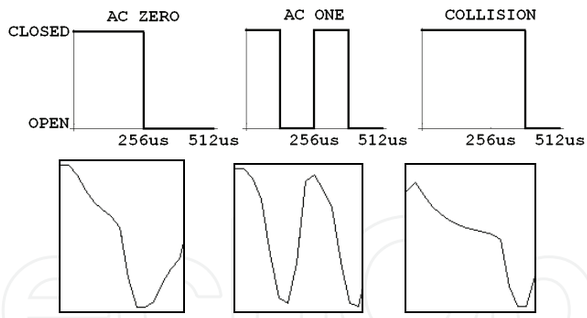

Fig. 13. The waveforms used by simulator for AC bit encoding via load modulation. The Y-axis indicates the state of the simulator switch. Below is shown the resulting baseband signal demodulated at the reader.

Via the RS232 interface of the Atmel board, a PC can program the tag simulator for performing various tasks. For instance, it can load the list of tag serial numbers into uC memory, set the number of tags participating to the simulation or choose the type of transponder to be simulated. In addition, the PC can program the simulator to perform tasks that would not be possible with a real tag, such as generating a sequence of load modulated pulses of a prescribed frequency or a single long pulse for determining the step response of the system antenna – reader.

The simulator can be a useful tool in the design of a reader, contributing to the visualization of transients and therefore to the choice of antenna Q according to what has been said in section 3.

6. Bit decoding for animal identification

In addition to the capability of tag identification with anticollision, our reader has been designed for data retrieval from single tags in Transponder Talk First (TTF) mode (NXP Semiconductors, 2006 b), which is used especially in animal identification. In contrast to the Reader Talk First (RTF) mode considered in section 2, where the tag sends data only following a reader request, in TTF mode the tag starts sending data as soon as it is powered by the antenna field. Data are sent continuously as long as power is maintained, the transmission of the last bit being followed by the retransmission of the first bit without pause between them. For the reader, this circumstance has the following implication. In RTF mode, the reader assumes that the start of the answer of the tag is separated from the end of the reader command by a known number of carrier cycles specified by the tag producer. This makes that bit boundaries are known to the reader. In TTF mode however, the reader has no indication about bit boundaries.

We shall describe in the following the procedure that is used in our reader for determining bit boundaries in TTF mode. The presentation of the principle will be clearer if we assume a continuous time axis instead of the discrete time imposed by sampling. We consider therefore a baseband signal $f(t)$ that Manchester encodes an infinite sequence of bits. The signal is formed by superposing translated copies of the basic waveform $w(t)$, which is defined as equal to 1 for $0 \le t < T/2$ and to –1 for $T/2 \le t < T$, where T is the bit duration. Specifically, $f(t) = \sum_{i=-\infty}^{\infty} c_i w(t - iT)$ where c_i equals 1 if the i-th bit is a one and -1 if the i-th

bit is a zero. Normally we would decode the i-th bit by computing the correlation $\frac{1}{T}\int_{-\infty}^{\infty} f(t)w_i(t)dt$ between $f(t)$ and the test function $w_i(t) = w(t - iT)$. However this would work only if the test functions w_i are aligned with the bit boundaries in the signal $f(t)$; this would no longer be the case if instead of $f(t)$ we would have a translated version $f(t - d_0)$. To align the test functions with the bit boundaries in the latter case, we proceed as follows. We compute the "moving correlations sums"

$$C(d) = \sum_{i=0}^{N-1} \left| \frac{1}{T}\int_{-\infty}^{\infty} f(t - d_0)w_i(t - d)dt \right|.$$

It turns out that the function $C(d)$ attains its maximum at d if and only if *either* the test functions $w_i(t - d)$ are aligned with the bit boundaries in f (that is, $d = d_0 + mT$ for some integer m) *or* they are displaced by half a bit duration with respect to bit boundaries in f (that is, $d = d_0 + T/2 + mT$ for some integer m) and all the N+1 bit waveforms in f whose supporting intervals intersect the union of the supporting intervals of $w_0(t - d)$, ..., $w_{N-1}(t - d)$ encode the same bit.

The proof of this result is very simple. Without narrowing generality we may assume $d_0 = 0$ and we may restrict our attention to the variation of $C(d)$ over $[0, T]$. In this situation, the supporting interval of $w_i(t - d)$ intersects only the bit intervals corresponding to bits i and i+1, so that $\left| \frac{1}{T}\int_{-\infty}^{\infty} f(t)w_i(t - d)dt \right|$ actually equals

$$\frac{1}{T}\left| c_i \int_{-\infty}^{\infty} w(t)w(t - d)dt + c_{i+1}\int_{-\infty}^{\infty} w(t - T)w(t - d)dt \right|.$$

As a function of d, the latter expression equals either $I(d)$ or $J(d)$ according to whether c_i coincides or not with c_{i+1}, the functions $I(d)$ and $J(d)$ being presented graphically in figure 14.

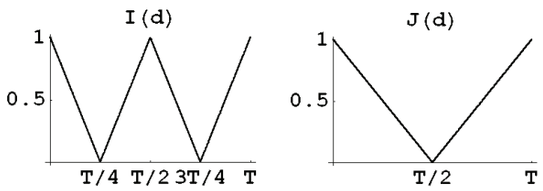

Fig. 14. The graphs of the functions $I(d)$ and $J(d)$.

It follows that $C(d)$ can be written as $kI(d) + (N - k)J(d)$, where k is the number of elements in the set $\{i \mid 0 \le i < N, c_i = c_{i+1}\}$. In case that bits 0 up to N all coincide, we have $k = N$ and we see from the graph of $I(d)$ that indeed it attains its maximum at 0, $T/2$ and T. If this is not the case, we have $k < N$; from the symmetry of graphs of I and J we may restrict ourselves to the interval $[0, T/2]$. We have to prove that $C(d) < C(0)$ for every d in that interval different from 0. This is certainly true if $0 < d \le T/4$ as both I and J are strictly decreasing on that interval. Now on the interval $[T/4, T/2]$ both I and J are linear and so is C, so that it suffices to prove that $C(T/2) < C(0)$; but this is immediate as $C(T/2) = k < N = C(0)$, which follows from the relations $I(0) = J(0) = 1$, $I(T/2) = 1$ and $J(T/2) = 0$.

We apply the described method in our reader as follows. Suppose we want to decode N bits transmitted by the tag and there are k samples per bit. We record in uC memory the samples for $N + 1$ bits, that is, $(N + 1)k$ samples. Then we compute the moving correlations sums as above, replacing the integrals by sums over discrete samples. Specifically, we start by computing the correlations for N bits as if the starting boundary of the first bit would be at the first recorded sample. Then we add together the absolute values of these correlations, which gives our first moving correlations sum. We memorize the decoding of N bits so obtained and the sum. Then we repeat the procedure, assuming now that the starting boundary of the first bit is situated at the second recorded sample, so that all correlations are computed starting from the second sample. We do this several times advancing by one sample, until we cover at least a bit interval; this is the reason of having recorded one bit in addition to the N required bits. Finally we estimate that the step that produced the maximal moving correlations sum among all computed sums gives the correct decoding of the N bits.

7. Conclusion

Low cost devices represent a significant trend of today's mass production, and the high competition places heavy demands on the ratio performance/price. We strived to face these demands by coming on the market with a design in which the non-standard usage of a chip allows one to obtain from it more than what was originally intended by the producer. We presented here tools and simulations that were useful to us in the design of the product.

8. References

Finkenzeller, K. (2003). *RFID Handbook*, John Wiley & Sons Ltd, ISBN 0-470-84402-7, West Sussex, England

Frosch Electronics (2004). *HITAG Long Range Reader Module HT RM801/901*. Available online at www.froschelectronics.com

Gelinotte, E., Frosch, R., Vuza, D.T. & Pascu, L. (2006). An RFID Reader Based on the Atmel AT91SAM7S64 Micro-Controller, *Proceedings of the 1st Electronics Systemintegration Technology Conference*, pp. 1158-1165, ISBN 1-4244-0552-1, Dresden, September 2006, Institute of Electrical and Electronics Engineers, Piscataway, NJ

NXP Semiconductors (2006 a). *HTRC110 Hitag Reader Chip*, Revision 3.0. Available online at www.nxp.com

NXP Semiconductors (2006 b). *Hitag S Transponder IC*, Revision 3.1. Available online at www.nxp.com

Vuza, D.T., Frosch, R. & Koeberl, H. (2007). A Long Range RFID Reader Based on the Atmel AT91SAM7S64 Micro-Controller, *30th ISSE 2007 Conference Proceedings*, pp. 445-450, ISBN 1-4244-1218-8, Cluj, May 2007, Institute of Electrical and Electronics Engineers, Piscataway, NJ

Development and Implementation of RFID Technology

Edited by Cristina Turcu

ISBN 978-3-902613-54-7
Hard cover, 450 pages
Publisher I-Tech Education and Publishing
Published online 01, January, 2009
Published in print edition January, 2009

The book generously covers a wide range of aspects and issues related to RFID systems, namely the design of RFID antennas, RFID readers and the variety of tags (e.g. UHF tags for sensing applications, surface acoustic wave RFID tags, smart RFID tags), complex RFID systems, security and privacy issues in RFID applications, as well as the selection of encryption algorithms. The book offers new insights, solutions and ideas for the design of efficient RFID architectures and applications. While not pretending to be comprehensive, its wide coverage may be appropriate not only for RFID novices but also for experienced technical professionals and RFID aficionados.

InTech Europe
University Campus STeP Ri
Slavka Krautzeka 83/A
51000 Rijeka, Croatia
Phone: +385 (51) 770 447
Fax: +385 (51) 686 166
www.intechopen.com

InTech China
Unit 405, Office Block, Hotel Equatorial Shanghai
No.65, Yan An Road (West), Shanghai, 200040, China
中国上海市延安西路65号上海国际贵都大饭店办公楼405单元
Phone: +86-21-62489820
Fax: +86-21-62489821

IntechOpen